90-223

+

объединенный
институт
ядерных
исследований
дубна

S17

E17-90-223

W.Salejda*

NUMERICAL STUDIES ON THE VIBRATIONAL SPECTRUM OF FIBONACCI CHAIN. A MULTIFRACTAL ANALYSIS

Submitted to "International Journal of Modern Physics B"

*On leave of adsence from Institute of Physics, Technical University of Wroclaw, Wybrzeze Wyspianskiego 27, 50 - 370 Wroclaw, Poland

1990

1. Introduction

Recently, a considerable amount of works has been devoted to studying anomalous scaling laws [1 - 3] of the energy spectrum (ES) of the Schrödinger equation [4-7], the one-dimensional quasi-periodic tight-binding models [8-11] and magnetic aperiodic chains [12-16].

On the other hand, the scaling properties of the vibrational spectrum of the system describing lattice dynamics of one - dimensional quasicrystals (1DQ) [17-24] are less investigated so far.

The aim of this paper is to perform the multifractal analysis (MA) of the ES of the harmonic Hamiltonian [19,21,23] modelling collective motions of atoms in the 1DQ [25,26].

In particular, we shall examine numerically the scaling behaviour of the normalized integrated density of states $\mathbb{G}$ in terms of scaling index α and fractal dimension f. The $\alpha - f$ spectra and Renyi dimensions $\mathbb{D}$ of the vibrational spectra (VS) will be calculated in a wide range of model parameters [21,23] using the algorithm developed in the theory of dynamic systems by Halsey et al. [1 - 2]. The next-nearest-neighbour interactions of atoms will be taken into account.

The paper is organized as follows. The considered model is specified in the next Section. The formalism of MA is described briefly in Sec.3. Numerical results are presented in Sec. 5. The last Section contains main conclusions.

2. Specification of the Harmonic Model

We consider the chain of N atoms with masses M the equilibrium positions l_n of which (in dimensionless form) are given by [21,23,25,26]:

$$l_n = n + [n / \sigma] / \sigma_g \tag{1}$$

where n are integer numbers, $\sigma_g = \sigma = (1+\sqrt{5})/2$ and [y] denotes the integer part of y .

The lattice dynamics of 1DQ is defined by the harmonic Hamiltonian [21,23]

$$H = \sum_{n=1}^{N} \frac{P_l^2}{2M} + \frac{1}{2} \sum_{n=1}^{N} \left(k_{n,n-1}(u_n - u_{n-1})^2 + g_{n,n-2}(u_n - u_{n-2})^2 \right), \quad (2)$$

where the standard symbols have been used [18,19,21,23].

We assume that the force constants of nearest-neighbour (NN) $k_{n,n-1}$ and next-nearest-neighbour (NNN) $g_{n,n-2}$ interactions depend on the distance between atoms and are given by quasiperiodic binary sequences [21,23]:

$$k_{n,n-1} = k_0 \left(1 + Q \left(1 - d_{n,n-1} \right) \right) \quad (3)$$

$$g_{n,n-2} = g_0 \left(1 + Q \left(2 - d_{n,n-2} \right) \right) \quad (4)$$

$$d_{n,n-i} = [\, n / \sigma \,] - [\, (n - i) / \sigma \,] \quad (5)$$

$$i = 1,2 \,,$$

where $Q = z/\sigma_g \geq 0$ is the parameter of quasiperiodicity (POQ); k_0 and g_0 denote spring constants of NN and NNN interactions, respectively.

In order to study the global scaling properties of the energy spectrum we shall examine the spectra of the model defined by Eqs. (2-5) for $\sigma = \eta_l = F_l / F_{l-1}$ [7,9], where $l=2,3,4 \ldots$ and F_l denotes the lth Fibonacci number with $F_0 = F_1 = 1$ and $F_l = F_{l-1} + F_{l-2}$.

For given rational approximants $\sigma = \eta_l$ to the golden mean σ_g the Fibonacci chain (1) is periodic. The length of the unit cell containing F_l atoms is equal to $L_l = a (F_l + F_{l-2})$ where a denotes the length of the shorter distance between atoms in the quasilattice (1). Therefore, the ES corresponding to $\sigma = \eta_l$ consists of F_l energy sub-bands and F_{l-1} gaps [7, 17].

Introducing now the mass dependent variables $\Psi_l(t)$ [27]:

$$u_l(t) = \sqrt{M}\, \Psi_l(t) = \sqrt{M}\, \Psi_l^0 \exp (i \omega t) \quad (6)$$

$$l=1,2,\ldots,N$$

and using the Bloch condition

$$u_{l+L_l} = \exp (i k L_l) u_l \quad (7)$$

the eigenvalue problem for the dynamic matrix (DM) $\mathbb{A}$ takes the form [21,23]:

$$\Omega^2 \vec{\Psi} = \mathbb{A} \vec{\Psi} , \quad (8)$$

where $\vec{\Psi} = (\Psi_1, \Psi_2, \ldots, \Psi_N)^T$, $\Omega^2 = M \omega^2 / k_0$ and

$$\mathbb{A} = \begin{pmatrix} a_1 & b_2 & c_3 & 0 & \cdots & 0 & c_1(k) & b_1(k) \\ b_2 & a_2 & b_3 & c_4 & 0 & \cdots & 0 & c_2(k) \\ c_3 & b_3 & a_3 & b_4 & c_5 & 0 & \cdots & 0 \\ & c_4 & b_4 & a_4 & b_5 & c_6 & 0 \cdots & 0 \\ & & & \cdots & \cdots & & & \\ & & & & \cdots & \cdots & & \\ c_1^*(k) & 0 & \cdots & & 0 & c_{N-1} & b_{N-1} & a_{N-1} \;\; b_N \\ b_1^*(k) & c_2^*(k) & 0 & \cdots & 0 & c_N & b_N & a_N \end{pmatrix} , \quad (9)$$

where

$$- b_n = 1 + Q - Q \left([n / \eta_l] - [(n - 1)/\eta_l] \right) \quad (10)$$

$$- c_n = h \left(1 + 2 Q - Q ([n / \eta_l] - [(n - 2)/\eta_l]) \right) \quad (11)$$

$$a_n = - (b_{n+1} + b_n + c_{n+2} + c_n) \quad (12)$$

and $c_1(k) = \exp(-ikL_l)c_1$, $c_1^*(k) = \exp(ikL_l)c_1$, $b_1(k) = \exp(-ikL_l)b_1$, $b_1^*(k) = \exp(ikL_l)b_1$, $c_2(k) = \exp(-ikL_l)c_2$, $c_2^*(k) = \exp(ikL_l)c_1$; $h = g_0/k_0$ denotes the strength of NNN interactions with respect to NN interactions.

3. Characterization of VS as Multifractal Objects

We describe briefly the formalism developed in Refs. [1, 2] and used in this paper.

Our aim is the quantitative estimation how bunched the eigenvalues Ω^2 of DM (cf. Eqs. (8)-(12)) on ES might be if $\sigma = \eta_l = F_l/F_{l-1}$ and l increases.

We characterize this bunching in terms of the scaling properties of the integrated (normalized to 1) density of states $G(x)$, where $x=\Omega^2/\Omega^2_{MAX}$ denotes the reduced square of the eigenenergy of the matrix $\mathbb{A}$. Notice that $0 \le \mathbb{G}(x) \le 1$ if $0 \le x \le 1$, i.e., it is non-negative and non-decreasing function of x on ES. Therefore, $\mathbb{G}$ can be treated as the measure [1-3].

We shall study the multifractal properties of the energy spectrum of DM on the basis of $\mathbb{G}(x)$. Let x and $x + \delta x$ both belong to ES. We say that $\mathbb{G}$ shows the local scaling at x with a scaling index α [7,8,17] if

$$\mathbb{G}(x + \delta x) - \mathbb{G}(x) \simeq (\delta x)^{\alpha} \tag{13}$$

as $\delta x \Rightarrow 0$.

We expect that α's will take a range of values between α_{min} and α_{max} . The density of singularities of type α on the interval (α_{min}, α_{max}) is determined by another index f defining also the fractal dimension of the subset of ES upon which the function $\mathbb{G}$ shows a local scaling law (13) [2,3].

In order to calculate the $\alpha - f$ spectrum we introduce the auxiliary quantity $\Gamma(q, \tau, P(\eta_1))$ [2] called the partition function

$$\Gamma (q, \tau, P(\eta_1)) = \sum_{i=1}^{F_1} \frac{(G_i)^q}{(w_i)^{\tau}}, \tag{14}$$

where $P(\eta_1)$ denotes the partition of ES obtained by the solution of (8) at $k = 0$ and $k_{max} = \pi/L_1$ [7]; w_i is the width of the ith energy sub-band the measure of which gives $G_i= 1/F_1$.

Solving now the equation

$$\lim_{l \Rightarrow \infty} \Gamma (q, \tau, P(\eta_1)) = 1 \tag{15}$$

we can obtain the $\alpha - f$ spectrum via a Legendre transformation

$$\alpha = d\tau(q)/dq \tag{16}$$

$$f = \tau(q) - q\,\alpha \tag{17}$$

and calculate in addition the Renyi dimensions $\mathbb{D} = D(q)$ [1-3,28]

$$\mathbb{D} = D(q)= \tau(q)/(q-1) \tag{18}$$

describing a measure of inhomogeneity in the bunching of eigenvalues Ω^2 of DM (9) on ES.

Notice that VS of the model under consideration are continuous if POQ is equal to zero. In this case, the α-f spectrum consists of two points: (1, $f(1)$=1) and (0.5, $f(0.5)$=0) corresponding to the center and the edges of spectrum, respectively.

If $z > 0$, then ES looks like Cantor set [17-19,23] and we expect that τ is a nonlinear function of q. In this case we are dealing with the anomalous scaling characterized by the infinite number of Renyi dimensions $\mathbb{D} = D(q)$ [1-3,28]. Therefore, we say that the ES is multifractal object with respect to function $\mathbb{G}$ the scaling behaviour of which describes an infinite number of scaling indices α distributed on the finite interval (α_{min} , α_{max}).

4. Numerical Results

We shall use the formalism presented in the previous Section to the calculation of $\alpha - f$ curves and the Renyi dimensions $\mathbb{D}$=D(q) of $\mathbb{G}(x)$.

In order to improve the convergence of our simulations, we have investigated numerically (instead of (15)) the equation [2]:

$$\frac{\Gamma (q, \tau, P(\eta_1,F_1))}{\Gamma (q, \tau, P(\eta_n,F_n))} = 1, \tag{19}$$

where $P(\eta_1,F_1)$ and $P(\eta_n,F_n)$ are the partitions of ES corresponding to the F_1 and F_n Fibonacci number, respectively.

On the basis of (19), the derivative $d\tau(q)/dq$ is given by

$$\frac{d\tau(q)}{dq} = \frac{S_1(q)\, \mathrm{Ln}\, r}{(r)^q\, S_3(q) - S_2(q)}, \tag{20}$$

where $S_1(q) = \sum_{i=1}^{F_1} (w_i)^{-\tau(q)}$, $S_2(q) = \sum_{i=1}^{F_1} \mathrm{Ln}(w_i)/ (w_i)^{\tau(q)}$,

F_n

$S_3(q)=\sum_{j=1} Ln(w_j)/(w_j)^{\tau(q)}$, $r=F_1/F_n$ and $\tau(q)$ is a solution of (19).

Let us point out that w_i (w_j) occurring in S_1, S_2, (S_3) denotes the quantity ($\Omega^2_{i+1} - \Omega^2_i$)/ Ω^2_{max} where Ω^2_{i+1} , Ω^2_i are the maximal and minimal eigenenergy in the ith sub-band; Ω^2_{max} is the maximal eigenvalue of DM (8). Thus, the argument of $\mathbb{G}$ is restricted to the interval <0,1>

We have solved numerically Eq. (8) at k=0 , $k=k_{max}$ and chosen values of $\sigma=\eta_1$ using a Dean algorithm [27,29,30].

Dependencies of τ, $d\tau/dq$ and $\mathbb{D}$ on q have been obtained by the numerical solution of (19). The α - f spectra have been calculated using (20) and eliminating q from Eqs. (16),(17).

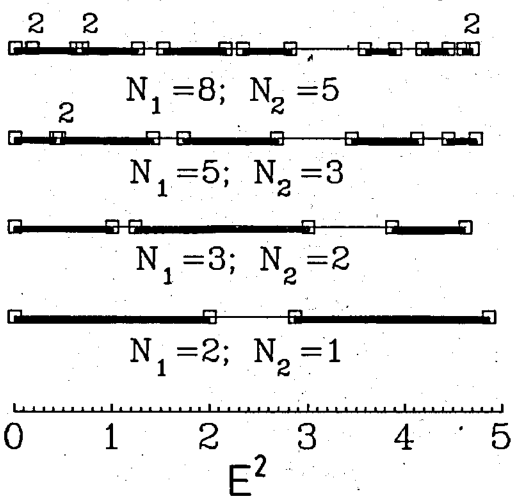

Fig. 1. Vibrational spectra at Q =0.7/σ'_g=0.7 F_{36}/F_{37}, h =0, $\sigma = \eta_l = F_l/F_{l-1} = N_1/N_2$ and l=2,3,4,5. The bold and thin lines correspond to sub-bands and gaps, respectively. Rectangular symbols represent eigenvalues Ω^2_i of (8) calculated at k=0 and $k=k_{max}$; the numbers over some symbols give the number of different Ω^2_i. On the abscissa the energetic scale in units of $E^2=M\omega^2/k_o$ is displayed.

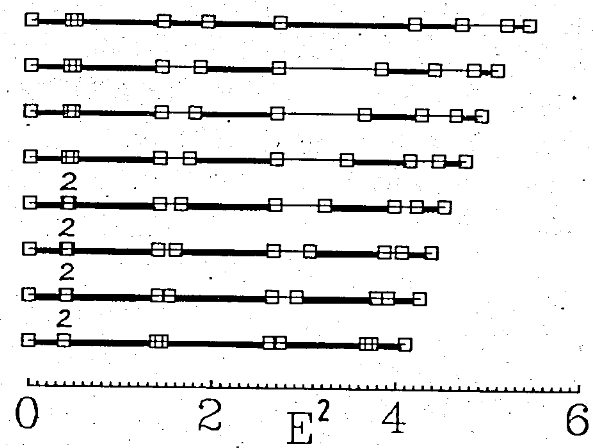

Fig. 2a. Vibrational spectra at $\sigma=\eta_4$=5/3, h=0, and increasing Q= z/σ'_g where z=0.1, 0.25, 0.5, 0.7, 0.85, 1.0, 1.3 and 2.5.

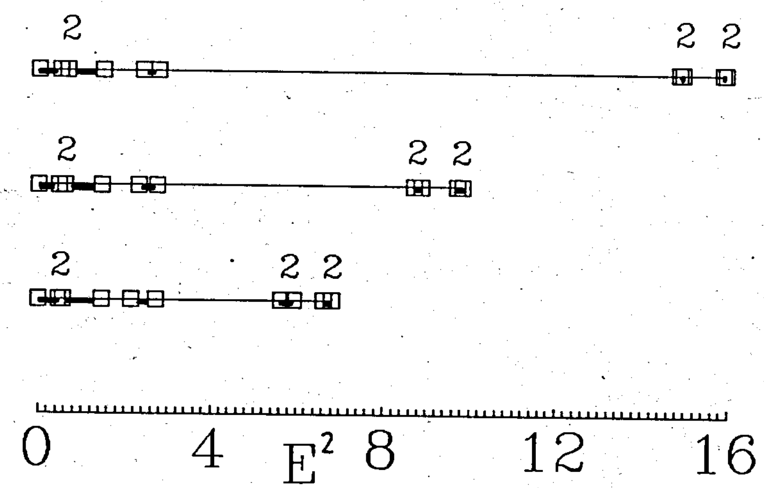

Fig. 2b. The same as in Fig. 2a at z = 5.0, 10.0 and 16.0.

In Fig. 1, the vibrational spectra of the model (2-5),(8-12) at h=0, Q=0.7/σ'_g , $\sigma'_g = F_{37}/F_{36}$, $\sigma = \eta_1 = F_1/F_{1-1}$ and increasing Fibonacci numbers F_1 are plotted.

Notice that the transformation of ES at $\sigma = \eta_1 \Rightarrow \sigma = \eta_{1+1}$ (cf. Fig. 1) exhibits the properties of the totally disconnected iterated function systems (IFS) [31] defined on the <0,1> interval.

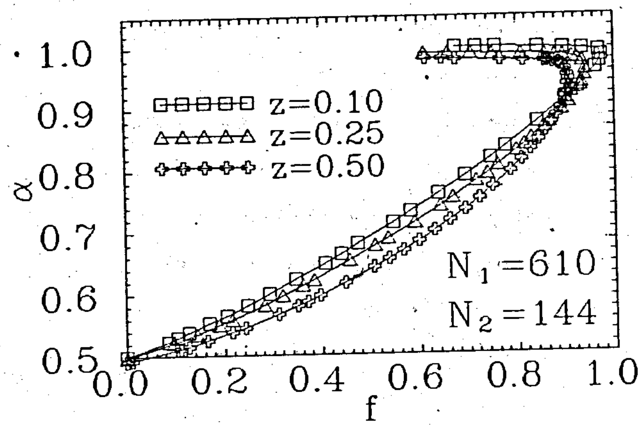

Fig. 3. The $f - \alpha$ spectra at h=0, N_1=F_{14}, N_2=F_{11} and depicted values of $Q = z/\sigma'_g$.

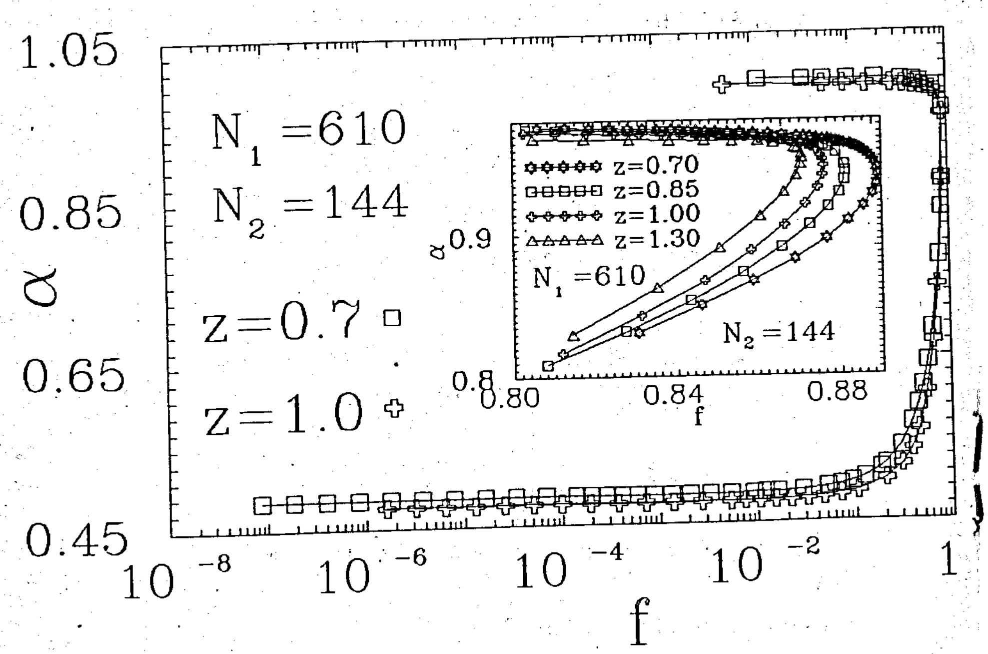

Fig. 4. The $f - \alpha$ spectra at h=0, N_1 =F_{14}, N_2 =F_{11} and indicated $Q = z/\sigma'_g$. Inset shows the top of $f(\alpha)$ curves.

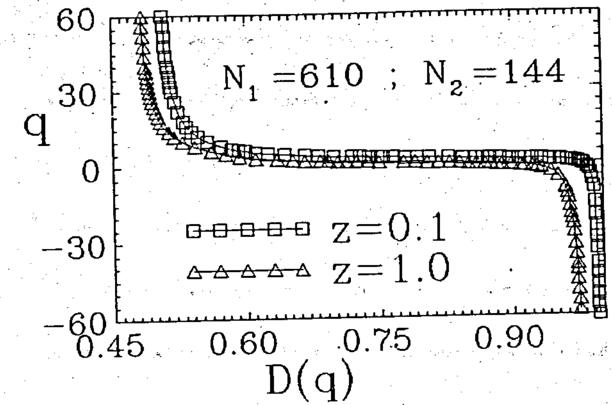

Fig. 5. Plots of the Renyi dimensions D=D(q) as a function of q at h=0, N_1 =F_{14}, N_2 =F_{11} and $Q=z/\sigma'_g$ where z=0.1, 1.0.

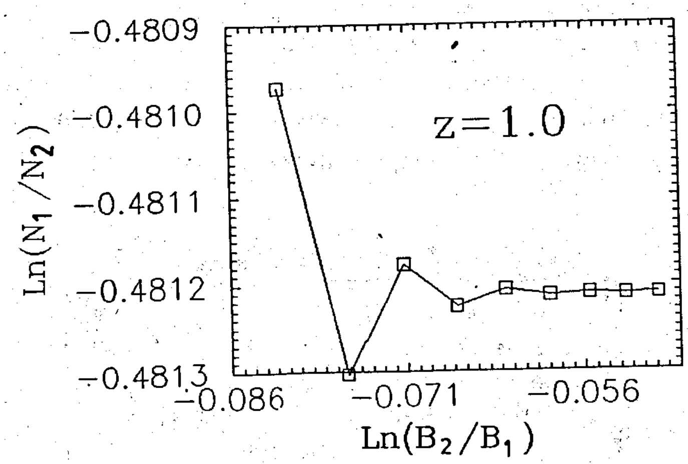

Fig. 6. The dependence of $\mathrm{Ln}(N_1/N_2)$ on $\mathrm{Ln}(B_2/B_1)$ at $Q = \sigma'_g$, N_1 = F_{l-1}, N_2=F_l, B_2=$\mathbb{B}_l$, B_1=$\mathbb{B}_{l-1}$ and l = 9, 10, ..., 17; $\mathbb{B}_l$ is the total width of ES corresponding to $\sigma=\eta_1 = F_l/F_{l-1} = N_2/N_1$.

It is a difficult problem to find the explicit form of contraction mappings defining this IFS since VS are inhomogeneous fractal objects (see below).

Vibrational spectra at $\sigma = \eta_4$, h = 0 and increasing values of Q are displayed in Fig.2 .

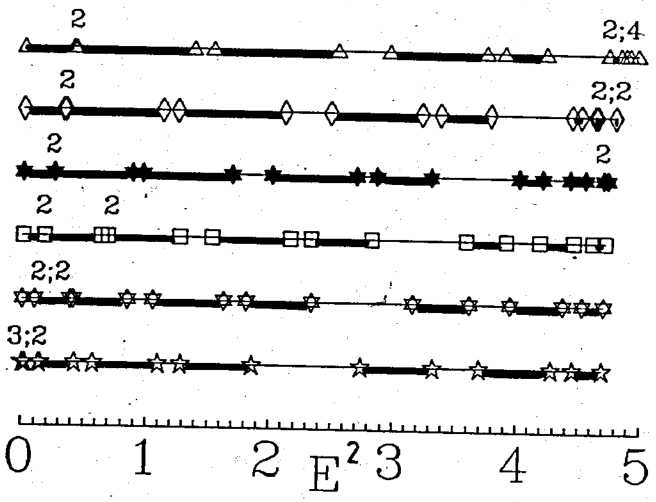

Fig.7. Vibrational spectra at $Q= 0.7/\sigma'_g$, $\sigma = \eta_5 = F_5/F_4$ and increasing h: (☆) h=-0.2, (✡) h=-0.1, (□) h=0.0, (✱) h=0.1, (◊) h=0.2, (△) h=0.3. The bold lines represent the energetic sub-bands; numbers over some symbols give the numbers of different eigenvalues of DM (8).

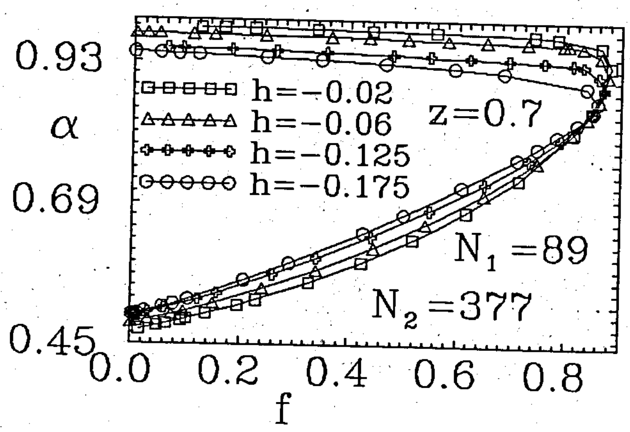

Fig.8. Plots of the f-α spectra at the depicted negative h and $Q= z/\sigma'_g$; $N_1=F_{10}$, $N_2=F_{13}$.

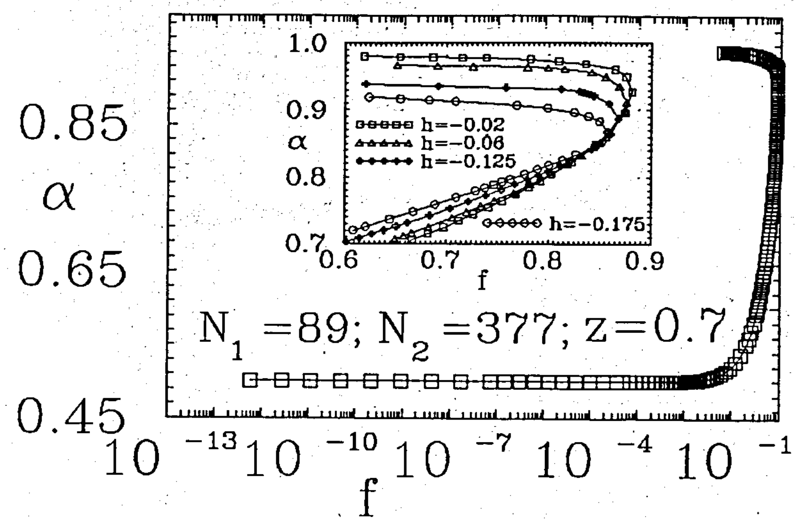

Fig.9. The f - α spectra at $Q=0.7/\sigma'_g$, $N_1 = F_{10}$, $N_2 = F_{13}$ and h = -0.125. Inset shows the top of $f(\alpha)$ curves at h = -0.02, -0.06, -0.125.

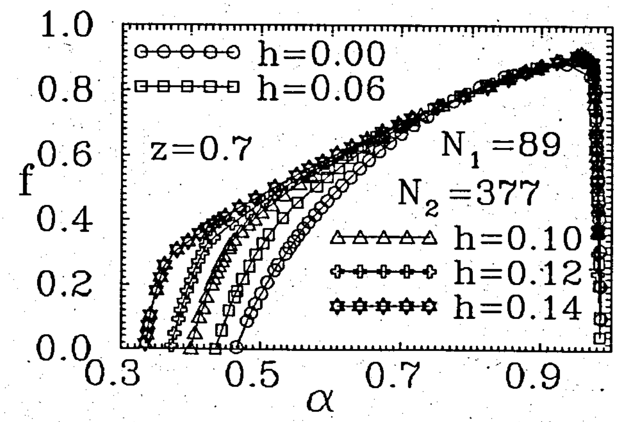

Fig.10. The α - f spectra at indicated $h \geq 0$, $Q=0.7/\sigma'_g$, $N_1 = F_{10}$ and $N_2 = F_{13}$.

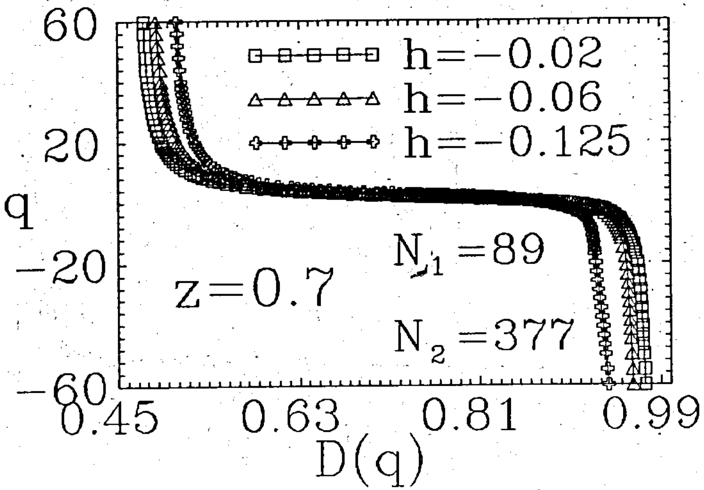

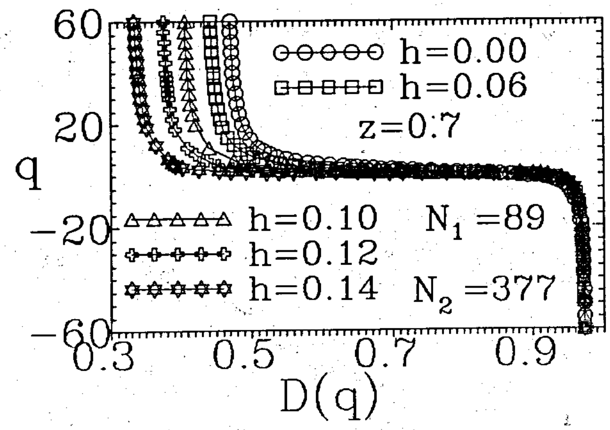

Fig. 11. Plots of $\mathbb{D} = D(q)$ as a function of q at $Q=0.7/\sigma'_g$, $N_1 = F_{10}$ and $N_2 = F_{13}$: (a) $h < 0$; (b) $h \geq 0$.

The α-f curves and $\mathbb{D}$ as a function of q at h=0, $N_1 = F_{14} = 610$, $N_2 = F_{11} = 144$ and rising magnitude of $Q = z/\sigma'_g$ are presented in Figs. 3, 4 and 5, respectively.

We have calculated also at $Q = 1/\sigma'_g$ and h=0 the index δ describing the dependence of the total energy bandwidth

$\mathbb{B}_1 = \sum_{n=1}^{F_1} w_n$ on the number of sub-bands F_1. We expect that $\mathbb{B}_1$ = const F_1^{δ} and $\delta = 1 - 1/D \simeq -\mathrm{Ln}(\mathbb{B}_1/\mathbb{B}_{1-1}) / \mathrm{Ln}(F_{1-1}/F_1)$ [7 - 9], where D is the fractal dimension of ES which is equal to $\mathbb{D}(q = 0) = f_{max}$. In Fig. 6 $\mathrm{Ln}(F_1/F_{1-1})$ as a function of $\mathrm{Ln}(\mathbb{B}_1/\mathbb{B}_{1-1})$ is plotted; notice that the difference $\mathbb{B}_1/\mathbb{B}_{1-1} - \mathbb{B}_{1-1}/\mathbb{B}_{1-2}$ (displayed on the abscissa) decreases with increasing 1.

The partitions of VS at $\sigma = \eta_5$, $Q = 0.7/\sigma'_g$ and growing h are presented in Fig. 7.

The α - f spectra and Renyi dimensions $\mathbb{D}$ as a function of q at $h \neq 0$, $N_1 = F_{13} = 377$ and $N_2 = F_{10} = 89$ are displayed in Figs. 8 - 10 and Fig. 11, respectively.

The dependence of the fractal dimension $D = \mathbb{D}(q = 0)$ of ES on h at $Q = 0.7/\sigma'_g$, $N_1 = F_{13}$ and $N_2 = F_{10}$ is plotted in Fig. 12.

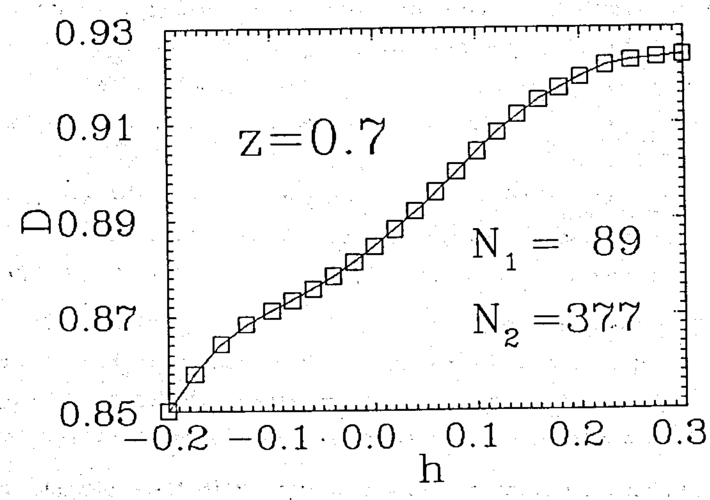

Fig. 12. The dependence of the fractal dimension $D = \mathbb{D}(q = 0)$ of ES on h at depicted $Q=z/\sigma'_g$; $N_1=F_{10}$ and $N_2=F_{13}$.

5. Conclusions and Final Remarks

The following conclusions result from the performed numerically MA:

1. Vibrational spectra of the harmonic model (2-5), (8-12) are inhomogeneous fractals [2,3] (cf. Figs. 3-5, 8- 11), i. e., they are multifractal objects with respect to the observable $\mathbb{G}(x)$ [3].

2. The dependencies of the Renyi dimensions $\mathbb{D}$ on q and α-f curves are smooth (cf. Figs. 5,11 and 4,9). The α-f spectrum of singularities of the integrated normalized density of states $\mathbb{G}$ is a well behaved function on the finite interval (α_{min} , α_{max}), where $\alpha_{min} = \mathbb{D}(q \Rightarrow +\infty)$, $\alpha_{max} = \mathbb{D}(q \Rightarrow -\infty) \simeq 1$ and $f(\alpha_{min}) = f(\alpha_{max}) = 0$.
   The $f(\alpha)$ curves are convex and reach their maximum f_{max} on $(\alpha_{min}, \alpha_{max})$ which is equal to the fractal dimension $D = \mathbb{D}(q=0)$ of the vibrational spectrum [9].

3. The form of the α-f spectra depends on the model parameters. In particular, we have observed the following tendencies:

3.1. The width of the interval $(\alpha_{min} = \mathbb{D}(q \Rightarrow -\infty)$, $\alpha_{max} = \mathbb{D}(q \Rightarrow +\infty))$ depends on the magnitude of model parameters and:
   - $\alpha_{min} = \mathbb{D}_{min} = \mathbb{D}(q \Rightarrow -\infty)$ decreases if $Q = z/\sigma'_g$ (cf. Figs. 3, 5) or h (cf. Figs. 8,10,11) is increasing;
   - $\alpha_{max} = \mathbb{D}_{max} = \mathbb{D}(q \Rightarrow +\infty) \Rightarrow 1$ independently of the magnitude of model parameters Q and h but $\partial\mathbb{D}(q)/\partial Q < 0$ (cf. Figs. 3,5) and $\partial D(q)/\partial h > 0$ (cf. Fig.8, inset in Fig.9 and Fig. 11).

3.2. The fractal dimension $D = \mathbb{D}(q = 0) = f_{max}$ of ES is a decreasing function of Q (cf. Fig.3 and inset in Fig. 4) and enlarges with h (cf. Figs. 8,11a, inset in Fig.9). These findings agree with the results of previous studies [23,32].

4. The fractal dimension D is connected with the index δ describing the scaling of the total widthband of ES $\mathbb{B}_1$ with the number of sub-bands [9]: $\mathbb{B}_1 \sim F_1^{\delta}$ and $\delta = 1-1/D$. Our numerical results obtained from maximum value f_{max} of the f-α curve (cf. Fig.3) and independently of the study of scaling of the total widthband $\mathbb{B}_1$ (cf. Fig.6) at $Q=0.7/\sigma'_g$, $N=F_{14}$ confirm this relation.

We point out that the multifractal analysis of VS can be performed using another measure, i.e., the normalized integrated density of states $\mathbb{F}(y)$ where $y = \Omega_i/\Omega_{max}$. We have verified numerically that the α - f spectra of $\mathbb{F}(y)$ and $\mathbb{G}(x)$ are qualitatively equivalent. The most remarkable differences betwen them have been noticed in these region of the α - f spectra where f takes its maximum. It follows from the obtained results that $f_{max}(\mathbb{G}) \simeq (f_{max}(\mathbb{F}))^2$ [23] where $f_{max}(\mathbb{G})$ and $f_{max}(\mathbb{F})$ denote the maximum value of f corresponding to the α - f spectra of $\mathbb{G}$ and $\mathbb{F}$, respectively.
In addition, we have observed that if instead of $\mathbb{G}$ the measure $\mathbb{F}$ is used then, the convergence of our simulations becomes less effective at $|q| \gg 1$.

Finally, let us comment on some aspects of our numerical studies.

During our simulations we have observed the double cusps in the plots of $f(\alpha)$ [33] at sufficiently large $|q|$ in two limiting cases: (I) at $Q < 0.1 / \sigma'_g$; (II) at $Q \geq 2.0 / \sigma'_g$.

The former one is connected with the tendency of the α-f spectra to attain the limit two-point spectrum (1,1), (0.5,0) corresponding to Q=0 [17].

In the latter case the breakdown of the scaling approach [1- 3] is the computer artifact since at sufficiently large Q the magnitude of sub-band widths w_i became very small (cf. Fig.2).

Notice that the convergence of the applied MA is less effective at $q \Rightarrow -\infty$ than at $q \Rightarrow +\infty$. This feature is visible in Figs. 4, 9 where the logarithmic scale has been applied to f.

It would be an interesting problem to study the multifractal properties of VS corresponding to another type of one-dimensional aperiodic crystals [34,35]. This will be the subject of separate investigations.

References

1. M.H.Jensen, L.P.Kadanoff, A.Libchaber, I.Procacia, J.Stavans, Phys. Rev. Lett. 55, 2798 (1985)
2. T.C.Halsey, M.H.Jensen, L.P.Kadanoff, I.Procacia, B.I.Shraiman, Phys. Rev. A33, 1141 (1986)
3. G.Paladini, A.Vulpiani, Phys. Rep. 156, 147 (1987)

4. M. Kohmoto, Phys. Rev. Lett. 51, 1198 (1983)
5. S.Ostlund, R.Pandit, Phys. Rev. B29, 1394 (1984)
6. M.Kohmoto, Y.Oono, Phys. Lett. 102A, 145 (1984)
7. C.Tang, M.Kohmoto, Phys. Rev. B34, 2041 (1986)
8. M.Kohmoto, B.Sutherland, C.Tang, Phys. Rev. B35, 1020 (1987)
9. S.N.Evangelou, J. Phys. C20, L295 (1987)
10. M.Holzer, Phys. Rev. B38, 1709 (1988)
11. M.Holzer, Phys. Rev. B38, 5756 (1988)
12. J.M.Luck, Th.M.Nieuwenhuizen, Europhys. Lett. 2, 257 (1986)
13. S.N.Evangelou, J. Phys. C20, L511 (1987)
14. M.Doria, I.Satija, Phys. Rev. Lett. 60, 444 (1988)
15. I.Satija, M.Doria, Phys. Rev. B38, 5174 (1988)
16. G.Györgyi, I.Satija, Phys. Rev. Lett. 62, 446 (1989)
17. J.M.Luck, D.Petritis, J. Stat. Phys. 42, 289 (1986)
18. J.P.Lu, T.Odagaki, J.L.Birman, Phys. Rev. B33, 4809 (1986)
19. F.Nori, J.P.Rodriques, Phys. Rev. B34, 2207 (1986)
20. S.E.Burkov, J. Stat. Phys. 47, 409 (1987)
21. W.Salejda, Commun. Joint Inst. Nucl. Res. E17-88-880, Dubna 1988
22. W.Salejda, Int. J. Mod. Phys. B3, 1109 (1989)
23. W.Salejda, Preprint Joint Inst. Nucl. Res. E17-89-281, Dubna 1989 (to be published in Acta Physica Polonica in 1990)
24. W.Salejda, Preprint Joint Inst. Nucl. Res. E17-89-538, Dubna 1989
25. D.Levine, P.J.Steinhardt, Phys. Rev. B34, 596 (1986)
26. J.E.S.Socolar, P.J.Steinhardt, Phys. Rev. B34, 617 (1986)
27. P.Dean, Rev. Mod. Phys. 44, 127 (1972)
28. A. Renyi, Probability Theory ,North Holland Publ. Comp., Amsterdam 1970; Chap.11
29. Z.Bo, J.Phys. A20, 6197 (1987)
30. W.Salejda, Commun. Joint Inst. Nucl. Res. E17-90-214, Dubna 1990
31. M. Barnsley, Fractals everywhere, Acad. Press, New York 1988; Chap.3
32. M.Valsakumer,G.Ananthahrishna J.Phys. C20, 9 (1987)
33. M.Wolf, J.Phys. A22, L1075 (1989)
34. J.M.Luck, Phys. Rev. B39, 5834 (1989)
35. J.E.S.Socolar, Phys. Rev. B39, 10519 (1989)

Received by Publishing Department
on March 30, 1990.